Cell

Characterizing Light-Regulated Retinal MicroRNAs Reveals Rapid Turnover as a Common Property of Neuronal MicroRNAs

Jacek Krol,[1] Volker Busskamp,[1] Ilona Markiewicz,[1] Michael B. Stadler,[1] Sebastian Ribi,[1,5] Jens Richter,[2] Jens Duebel,[1] Silvia Bicker,[3] Hans Jörg Fehling,[4] Dirk Schübeler,[1] Thomas G. Oertner,[1] Gerhard Schratt,[3] Miriam Bibel,[2] Botond Roska,[1,*] and Witold Filipowicz[1,*]

[1]Friedrich Miescher Institute for Biomedical Research, PO Box 2543, 4002 Basel, Switzerland
[2]Neurodegeneration Department, Neuroscience Research, Novartis Institutes for Biomedical Research, 4002 Basel, Switzerland
[3]Interdisziplinäres Zentrum für Neurowissenschaften, Universität Heidelberg, and Institut für Neuroanatomie, Universitätsklinikum Heidelberg, Heidelberg, Germany
[4]Institute of Immunology, University Clinics Ulm, Germany
[5]Present Address: Fisher Clinical Services GmbH, 4123 Allschwil, Switzerland
*Correspondence: botond.roska@fmi.ch (B.R.), witold.filipowicz@fmi.ch (W.F.)
DOI 10.1016/j.cell.2010.03.039

SUMMARY

Adaptation to different levels of illumination is central to the function of the retina. Here, we demonstrate that levels of the miR-183/96/182 cluster, miR-204, and miR-211 are regulated by different light levels in the mouse retina. Concentrations of these microRNAs were downregulated during dark adaptation and upregulated in light-adapted retinas, with rapid decay and increased transcription being responsible for the respective changes. We identified the voltage-dependent glutamate transporter *Slc1a1* as one of the miR-183/96/182 targets in photoreceptor cells. We found that microRNAs in retinal neurons decay much faster than microRNAs in nonneuronal cells. The high turnover is also characteristic of microRNAs in hippocampal and cortical neurons, and neurons differentiated from ES cells in vitro. Blocking activity reduced turnover of microRNAs in neuronal cells while stimulation with glutamate accelerated it. Our results demonstrate that microRNA metabolism in neurons is higher than in most other cells types and linked to neuronal activity.

INTRODUCTION

The first steps of vertebrate visual processing occur in the retina (Wässle, 2004). Light is converted to neural signals by photoreceptors, the more sensitive rods and the less sensitive cones, which can adapt to several log unit changes in intensity, enabling the rest of the visual system to remain responsive over an intensity span of ~8 log units. Information flows from photoreceptors to bipolar cells and then to ganglion cells, which then communicate with higher brain centers. The transfer of information from photoreceptors to bipolar cells is modified by the inhibitory horizontal cells in the outer plexiform layer (OPL), and from bipolar to ganglion cells by the inhibitory amacrine cells in the inner plexiform layer (IPL). The cell bodies of these neurons are located in distinct retinal layers: photoreceptors in the outer nuclear layer (ONL); bipolar-horizontal-amacrine cells in the inner nuclear layer (INL); and amacrine and ganglion cells in the ganglion cell layer (GCL).

Adaptation to different light levels in the retina occurs on a timescale ranging from milliseconds to hours depending on the mechanism involved. The most-studied cellular site of light-dark adaptation are the photoreceptors, where both the light-sensing (Fu and Yau, 2007) and adaptation machinery have been described in detail (Pugh et al., 1999). In addition, different light-dark adaptation phenomena have also been noted in other cellular components of the retinal network, proximal from photoreceptors, in the INL and GCL (Demb, 2008). The coordination and regulation of the molecular network in different states of light-dark adaptation is not well understood. In this work, we investigated whether the process of light-dark adaptation in the mouse retina involves microRNAs (miRNAs). The layered organization of the retina and the fact that retinal cells activity can be controlled in vivo by light, the physiological input, make the retina a good model to study miRNAs regulation in neural circuits.

In mammals, miRNAs generally base-pair imperfectly to sequences in the 3′-untranslated region (UTR) of target mRNAs and repress protein synthesis, either by inhibiting translation of mRNAs or causing their destabilization (Filipowicz et al., 2008; Bartel, 2009). miRNAs are implicated in the control of many fundamental processes and most miRNAs are expressed in a development- or tissue-specific manner (Bushati and Cohen, 2007; Bartel, 2009). In particular, many miRNAs are specifically expressed or enriched in neuronal cells, including those of the retina (Arora et al., 2007; Karali et al., 2007; Loscher et al., 2007; Xu et al., 2007), consistent with growing evidence of importance of miRNAs for brain development and function (Kosik, 2006; Schratt 2009).

Hundreds of different miRNAs have been characterized in mammals. They are either encoded by independent genes or are excised from introns. During miRNA processing, primary transcripts (pri-miRNAs) are first cleaved in the nucleus to ~70-nt-long pre-miRNA hairpins, which are then matured in the cytoplasm to miRNAs (Ding et al., 2009). Although details of miRNA biogenesis and its regulation are quite well established, little is known about catabolism of miRNAs. They are generally assumed to have a very long half-life, corresponding to many hours or even days (Bhattacharyya et al., 2006; Hwang et al., 2007; Gatfield et al., 2009). However, such a slow turnover may not be a universal feature of miRNAs since they often play a role in rapid developmental transitions or act as on and off switches, conditions which call for a more active miRNA metabolism (Bushati and Cohen, 2007; Bartel, 2009).

We found that a subset of miRNAs is reversibly up- and downregulated in vivo in the retina during light-dark adaptation, independent of the circadian rhythm. The sensory neuron-specific miR-183/96/182 cluster, and miR-204 and miR-211, are downregulated during dark adaptation and upregulated in light, with rapid miRNA decay and increased transcription being responsible for the changes. One of the identified targets of the light-regulated miRNAs, *Slc1a1*, might fine-tune synaptic function in different light-adaptation states. Finally, we found that fast turnover of many miRNAs is not limited to the retina but is a general property of neurons, and that activity is an important regulator of miRNA turnover in neurons.

RESULTS

miRNAs Expressed in Dark- and Light-Adapted Mouse Retina

We characterized populations of small RNAs isolated from retinas of mice adapted to either light or dark (see Extended Experimental Procedures online). To obtain a global picture of small RNAs expressed in these two conditions, cDNA libraries of gel-purified small RNAs were subjected to deep sequencing using the 454 methodology. Analysis of ~75,000 reads identified 253 retinal miRNAs expressed in either dark-adapted (DA) or light-adapted (LA) states (Figure S1A; Table S1). miRNAs, whose levels increased in LA retina included those encoded by the intergenic miR-183/96/182 cluster and intronic miRNAs miR-204 and -211 (Figures 1A and 1B; Table S1), identified previously as being expressed in the retina (Ryan et al., 2006; Karali et al., 2007; Loscher et al., 2007; Xu et al., 2007). Two other platforms were also used to globally assess the effect of light on miRNA levels in the retina: Exiqon arrays and Illumina deep sequencing. A light-induced increase in the level of miR-183/96/182 cluster miRNAs was seen in two independent array experiments, while increases in miR-204/211 was only detected in one (Figure 1A; Table S1). The Illumina sequencing did not yield consistent results. In one experiment, miR-96, -204, and -211 (but not miR-182 and -183) were upregulated 1.5- to 2.5-fold in LA retina, but in another experiment no stimulatory effect was observed (data not shown); possibly, ~2-fold effects are too small to be reproducibly quantified by this method. To quantify miRNA levels by other, more direct techniques, the light-dependent changes in selected miRNAs were determined by quantitative real-time PCR (qRT-PCR) and RNase protection assays (RPA). These analyses demonstrated that expression levels of miRNAs encoded by the miR-183/96/182 cluster, and miR-204 and -211, increased 1.5- to 2.5-fold in LA retina (Figures 1C and 1D). Since a light-induced increase in the level of these miRNAs was detected by at least three independent methods, they were selected for further analysis (for comparable changes in expression of these miRNA ascertained by still another independent method, see below). It should be noted that both 454 and Exiqon I analyses identified light-dependent changes in a number of miRNAs other than miR-183/96/182, and miR-204 and -211. Since these changes were not confirmed by other analyses, these miRNAs were not further investigated. The levels of miRNAs let-7b and miR-29c (Figures 1A, 1C, and 1D) did not change significantly in any analyses, and these miRNAs were therefore used as controls.

The miR-183/96/182 cluster miRNAs have related seed sequences, while the seeds of miR-204 and -211 are identical. The latter two miRNAs are excised from introns of two related protein-coding genes, *Trpm3* and *Trpm1*, which are expressed in the retina (Figure 1B; see also Figure S2B). Since the levels of miR-183/96/182 miRNAs have been reported to vary ~2-fold during the day (Xu et al., 2007), we verified that the alterations observed by us were not due to changes in gene expression associated with the circadian rhythm. For the miR-183/96/182 cluster and other miRNAs tested, increased accumulation upon light adaptation occurred independently of whether the measurements were performed at noon (Zeitgeber [ZT] 6) or at midnight (ZT18) (Figures S1B and S1C).

Expression of miRNAs in Different Retina Layers

To establish expression patterns of the miRNAs investigated in different retinal cell layers we used laser capture microscopy (LCM) to dissect the LA and DA retinas. The quality of the LCM dissection was verified by demonstrating that captured samples were enriched in mRNAs known to be expressed in specific retinal cells (Figure S2C). RNA was isolated from three different layers: a layer containing photoreceptor cells (ONL+OS/IS); INL; and GCL. These were analyzed by qRT-PCR (Figure 1E), revealing that miRNAs of the miR-183/96/182 cluster were most abundant in photoreceptors, while miR-204 and −211 were enriched in the INL. The levels of miR-183/96/182 miRNAs in the ONL+OS/IS layer and miR-204 and -211 in the INL increased in response to light, consistent with the data obtained for a whole retina captured by LCM (Figure 1F). Levels of miR-183/96/182, miR-204, and -211 in the GCL were very low, although the level of a brain-specific miRNA, miR-124a, was comparable to that in other cell layers (Figure 1E).

Enrichment of the investigated miRNAs in different retinal layers was confirmed by in situ hybridizations (ISH) performed on sections from LA retina. In photoreceptors, strong signals were detected with probes specific for miR-182, -183, and -96, but not with the respective mutant probes (Figure S1D). Weaker signals for miR-182, -183, and -96 were also detected in the INL (Xu et al., 2007). In contrast, the INL stained strongly with probes for miR-211 and let-7b (Figure S1D). None of the used probes detected substantial levels of miRNAs in ganglion cells, consistent with the LCM data.

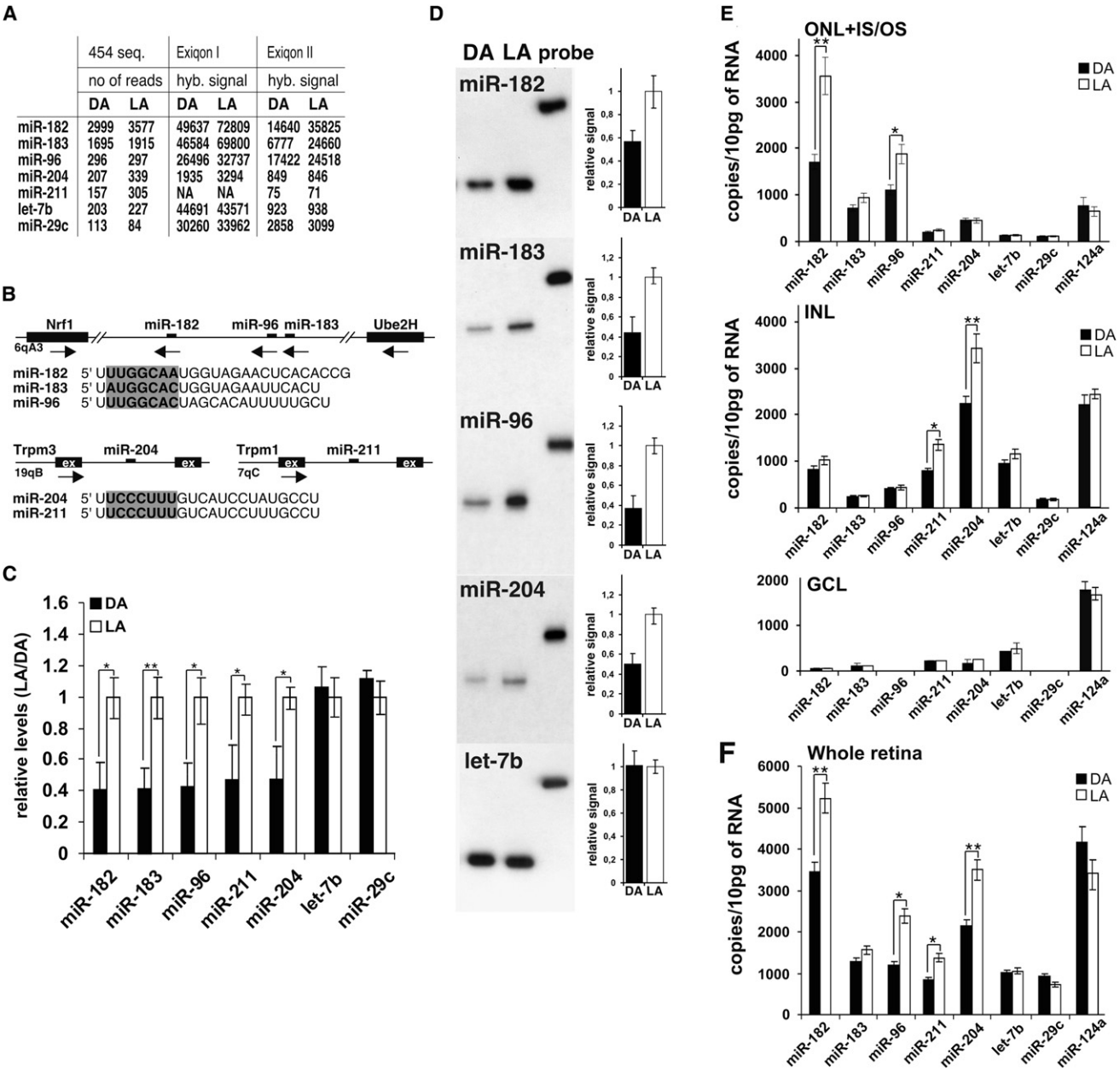

Figure 1. Differences in miRNA Levels between LA and DA Retinas

(A) Number of reads determined by 454 sequencing and Exiqon array hybridization signals (from two independent experiments) for selected miRNAs expressed in DA and LA retinas. NA, signal intensity close to background.

(B) Schemes of genomic organization of the intergenic miR-183/96/182 cluster, and intronic miRNAs miR-204 and -211. Genes or exons flanking miRNA sequences, and chromosomal positions are indicated. Sequences of mature miRNAs are shown below, with seeds highlighted.

(C) Comparison of miRNA levels in DA (black bars) and LA (white bars) retinas by qRT-PCR. The values, normalized for U6 RNA, are means ± SEM (six independent experiments [n = 6]); *$p < 0.05$, **$p < 0.01$. Values for LA retinas are set to one.

(D) Quantification of selected miRNAs by RPA. The graphs show phosphorimaging quantification of miRNA levels (means ± SEM; n = 5).

(E and F) miRNA levels in LCM-dissected layers of DA and LA retina (E) or a whole retina (F). Values, normalized for U6 RNA, are means ± SEM (n = 3).

See also Figure S1 and Table S1.

Identification of Potential Targets of miR-183/96/182 Cluster miRNAs

To gain an insight into the biological role of miRNAs undergoing light-induced changes in the retina, we compiled a list of potential targets of miRNAs from the highly expressed miR-183/96/182 cluster, using three computational target prediction algorithms: TargetScan 5.1 (www.targetscan.org); MicroCosm (www.microrna.sanger.ac.uk); and PicTar

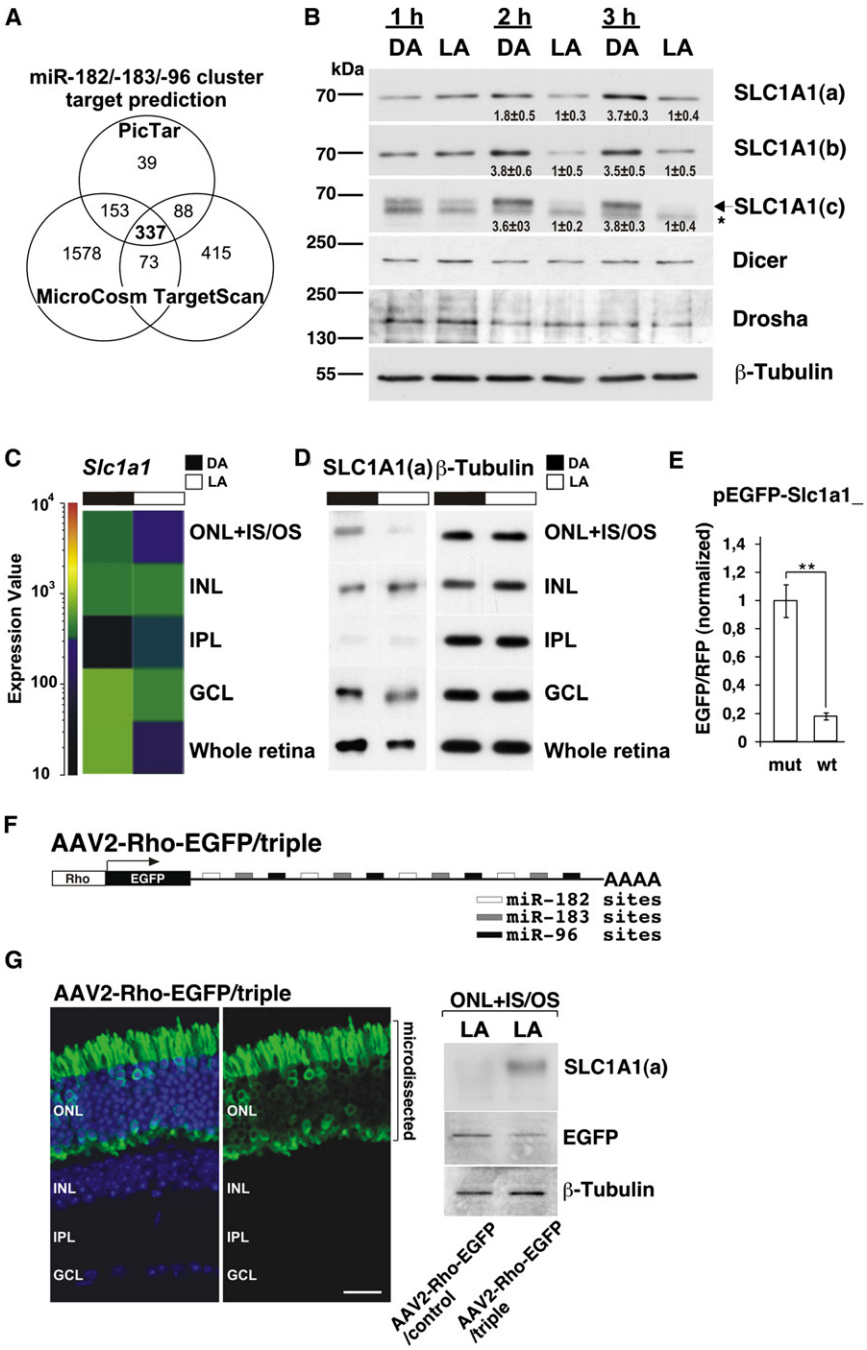

Figure 2. Glutamate Transporter *Slc1a1* Is Targeted by miR-183/96/182 miRNAs

(A) Venn diagram showing targets of miR-183/96/182 cluster predicted by PicTar, Targetscan 5.1, and MicroCosm algorithms.

(B) Western analysis of protein lysates of LA retinas and retinas from mice adapted to dark (DA) for 1, 2, or 3 hr, using three different (a through c) anti-SLC1A1 Abs, and Abs against Dicer, Drosha, and β-Tubulin. Asterisk, nonspecific band recognized by SLC1A1(c) Ab. Increase in the intensity of SLC1A1 bands in DA retinas at 2 and 3 hr of dark adaptation (always calculated relative to levels in LA retinas) is indicated. Values are means ± SEM from three westerns performed with each Ab.

(C) The heat map comparing *Slc1a1* mRNA levels, as assessed using Affymetrix arrays and related to median expression values, in different LCM-dissected layers of DA and LA retinas.

(D) Western blot analysis of lysates of different layers (~100,000 cells/layer) of DA and LA retinas, using anti-SLC1A1(a) and anti-β-Tubulin Abs.

(E) Two-photon ratiometric imaging of EGFP expression from pEGFP-Slc1a1_wt and _mut constructs electroporated, together with a reference pDsRed plasmid to photoreceptors in vivo. The graphs show relative ratios of EGFP to RFP signals (measured for 20 individual cells for each combination of plasmids), with the ratio for pEGFP-Slc1a1_mut set to 1.0. Values are means ± SEM.

(F) Scheme of the AAV-Rho-EGFP-triple sponge, harboring four sites for each of the miR-183/96/182 miRNAs.

(G) *(left panel)* Confocal cross section of an immunostained LA retina infected with AAV2-Rho-EGFP/triple. Left and right pictures visualize EGFP plus DAPI and EGFP alone, respectively. *(right panel)* Western analysis of lysates from five combined ONL+OS/IS layers of retinas infected with either AAV2-Rho-EGFP/triple or control sponge.

See also Figure S2, Figure S3, and Table S2.

(www.pictar.mdc-berlin.de). Of the potential targets bearing miR-183/96/182 binding sites in the 3′-UTR, 337 were predicted by all three algorithms (Figure 2A). 214 of them are expressed in mouse retina (Table S2). We used RNA isolated from retina cell layers obtained by LCM to profile mRNA expression using Affymetrix arrays. For 12 gene transcripts predicted as potential targets of miR-183/96/182 miRNAs, we observed enrichment of more than 2.0-fold ($p < 0.05$) in the ONL+OS/IS photoreceptor layer of DA retina as compared to LA retina (Figure S2A; Table S2). Among the aforementioned twelve mRNAs are those encoding a sodium/potassium-transporting ATPase subunit ATP1B3, a voltage-dependent glutamate transporter SLC1A1, and a polyA-binding protein interacting protein 2B (PAIP2B, a translational inhibitor). The expression of *Trpm1* and *Trpm3* genes, hosting miR-211 and -204 in their introns, was generally increased in a whole retina or its layers upon exposure to light, although in most instances the changes were not statistically significant (Figure S2B). This regulation is of potential interest since TRPM1 was recently implicated in the signal transduction in retinal ON bipolar cells (Morgans et al., 2009; Shen et al., 2009).

Validation of Selected Targets of miR-183/96/182 Cluster miRNAs

The gene encoding the voltage-dependent glutamate transporter, SLC1A1, was first selected for a more detailed analysis. Glutamate transporters are responsible for scavenging glutamate from the synaptic cleft after release (Nieoullon et al., 2006; Tzingounis and Wadiche, 2007). Western blot analysis performed with extracts of DA and LA retinas, and three different antibodies recognizing distinct sequences of SLC1A1, revealed that the level of the protein increased by up to 3.8-fold following 2- or 3 hr adaptation to dark, an effect expected to accompany the decrease in miR183/96/182 levels in the dark. No light-dependent changes were observed in the levels of several control proteins, including Drosha and Dicer (Figure 2B). Importantly, analysis of different LCM-dissected layers revealed a marked increase in both *Slc1a1* mRNA and protein levels in the photoreceptors of DA retina (Figures 2C and 2D).

Different approaches were used to demonstrate that SLC1A1 is a direct target of miR-183/96/182 miRNAs. We constructed enhanced green fluorescent protein (EGFP) and firefly luciferase (FL) reporters containing either wild-type (wt) full-length *Slc1a1* 3′-UTR or the 3′-UTR bearing mutations in seed sequences of the two predicted sites recognized by miR-183/96/182 miRNAs (Figure S3A). When transfected into mouse NIH 3T3 cells, both types of wt, but not mutant, reporters were inhibited by miRNA mimics specific for individual miR-183/96/182 miRNAs, cotransfected either individually or as a mixture of all three (Figures S3B and S3G).

To find out if the EGFP reporter is similarly regulated in a more physiological context and in response to endogenous miRNAs, the wt (pEGFP-Slc1a1_wt) and mutant (pEGFP-Slc1a1_mut) EGFP reporters were in vivo electroporated into retinas of newborn mice to mostly target photoreceptors (Matsuda and Cepko, 2004). The coelectroporated reporter expressing red fluorescent protein (RFP) was used as a normalization control. EGFP and RFP fluorescence in individual photoreceptor cells from electroporated retinas (>21 days postelectroporation) was measured by two-photon live microscopy. Activity of the EGFP reporter containing wt miRNA sites was found to be ~5-fold lower than that of the mutated form (Figure 2E). No significant difference was found in the levels of EGFP between LA and DA retinas electroporated with pEGFP-Slc1a1_wt (data not shown); possibly, electroporation of newborn mouse retinas affects proper light regulation of miRNA expression in photoreceptors.

To get further support for the role of the miR-183/96/182 cluster in regulating *Slc1a1* mRNA, we generated EGFP constructs expressing miR-183/96/182-specific "sponges" in their 3′-UTR (Ebert et al., 2007). Three sponges, each containing eight sites complementary to one of the three miR-183/96/182 cluster miRNAs and a sponge containing four sites specific to each of the three miRNAs (triple sponge) were constructed (Figures S3C–3F). When tested in mouse NIH 3T3 cells, all sponges markedly relieved the repression of FL-Slc1a1_wt reporter induced by the cotransfection of either single miR-183/96/182 cluster miRNAs or a mixture of the three (Figure S3G).

We chose adeno-associated virus (AAV)-mediated gene transfer to deliver the triple sponge into photoreceptors in vivo. The sponge sequence was cloned into the 3′ UTR of an EGFP cDNA, whose expression is driven by the human rhodopsin (Rho) promoter, yielding AAV2-Rho-EGFP/triple (Figure 2F). The untagged EGFP AAV construct, AAV2-Rho-EGFP/control, served as a control. AAV particles were administrated subretinally, the sponged AAV into one eye and the control AAV into the contra-lateral eye of the same adult mice ($p > 42$). Infected retinas were isolated three weeks post-AAV injection and their EGFP-expressing ONL+OS/IS layers were dissected by LCM (Figure 2G). Western blot analysis revealed that infection with AAV-Rho-EGFP-triple resulted in a marked increase in the SLC1A1 protein level when compared to retinas infected with AAV-Rho-EGFP-control (Figure 2G), indicating that *Slc1a1* is a direct target of the miR-183/96/182 cluster. Of note, expression of the triple sponge had no effect on the level of targeted miRNAs (Figure S2G).

Western analysis of extracts from DA and LA retinas, and from "sponged" ONL+OS/IS layers with antibodies specific for PAIP2 and ATP1B3, two other predicted miR-183/96/182 targets (Figures S2A and S2D), revealed that levels of these proteins are ~2-fold higher in DA retinas and in photoreceptors cells expressing the AAV-Rho-EGFP-triple sponge (Figures S2E and S2F). Hence, similarly to *Slc1a1*, also *Paip2b* and *Atp1b3*, likely represent direct targets of the miR-183/96/182 cluster in photoreceptors.

Kinetics of Light-Dependent Changes in miRNA and Pri-miRNA Levels

miRNAs are known to generally have a slow turnover (Bhattacharyya et al., 2006; Hwang et al., 2007; Gatfield et al., 2009; see also below). Our finding that the abundance of many retinal miRNAs markedly decreased following 3 hr in the dark (Figure 1) was therefore unexpected, and prompted us to measure the kinetics of changes in miRNA levels in response to dark and light adaptation. Following transfer of mice to the dark, levels of miR-183/96/182, and miR-204 and -211, reached their minimum after approximately 90 min. However, upon return to light following dark adaptation for 3 hr, the miRNAs reached maximal levels after only 30 min. No significant changes were seen in the levels of let-7b and miR-29c (Figure 3A and Figure S4A).

The kinetic data indicated that the more prolonged decrease in miRNA levels might be due to miRNA decay, while the rapid increase could result from augmented transcription and RNA processing. Generally (for exceptions, see Ding et al., 2009), processing of pri- and pre-miRNAs is quite rapid, and assessment of their levels provides an approximate measure of miRNA gene transcription. Analysis of pri-miRNAs using qRT-PCR revealed that changes in their levels indeed occur relatively fast ($\leq$30 min), irrespective of the animals being transferred from light to dark (decreased levels) or dark to light (increased levels) (Figure 3B and Figure S4B). Similar results were obtained when combined levels of both pri- and pre-miRNAs were analyzed using RT-PCR (Figures S4C and S4D). Quantification of pri- and pre-miRNA suggests that changes in the level of light-induced miRNAs are a consequence of transcriptional upregulation of their genes in response to light. These measurements, performed by procedures different from those presented in

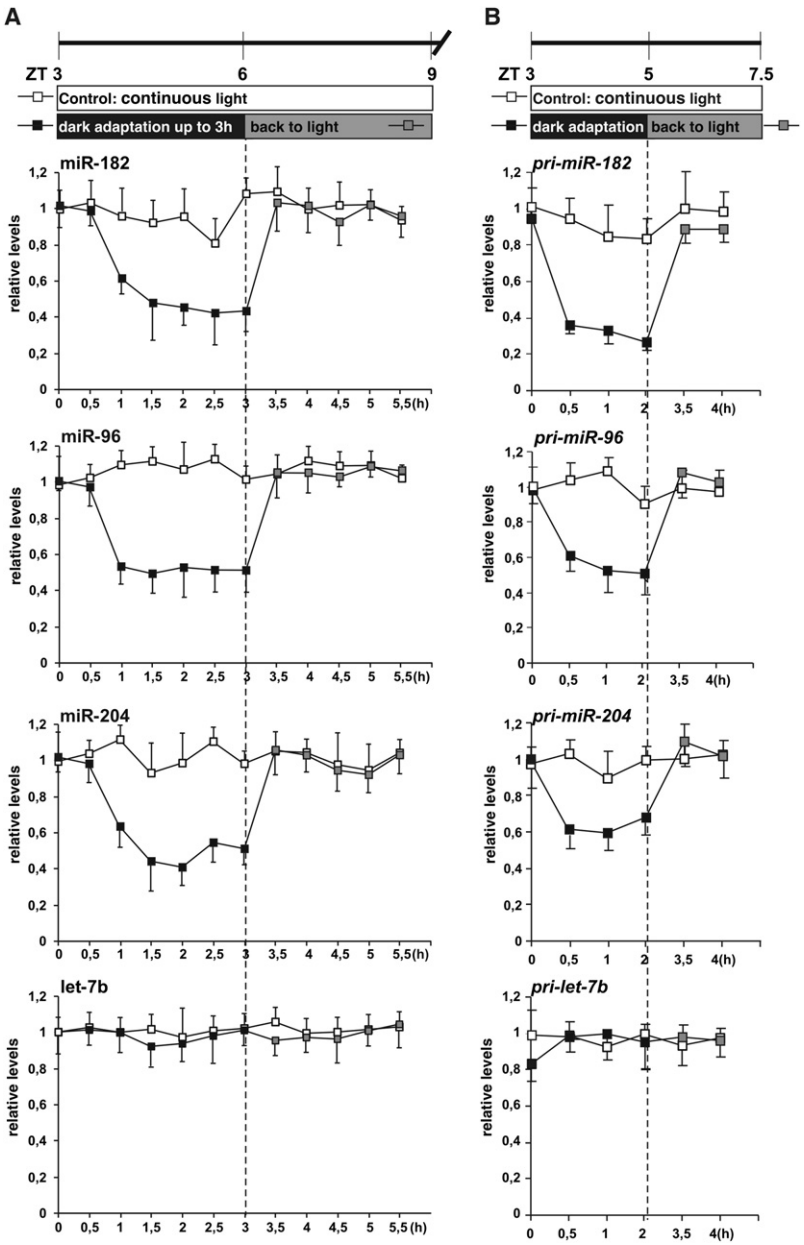

Figure 3. Kinetics of Changes in Mature miRNA (A) and Pri-miRNA (B) Levels in Retina during Adaptation to Dark and Light

Schemes at the top describe light/dark adaptation regime. Values, normalized to U6 RNA, represent means ± SEM; n = 2. Values for LA retinas at 0 hr were set to one. See also Figure S4.

Figure 1, also provide independent evidence that the expression of the investigated miRNA genes differs between LA and DA retinas.

Inhibitor Assays Reveal Rapid Turnover of miRNAs in Retina

We used specific inhibitors to directly test whether transcription is responsible for the upregulation of precursor and mature forms of miR-183/96/182, miR-204, and miR-211. Transcription inhibitors, actinomycin D (ActD) or α-amanitin (α-Am), were injected intraocularly into the right eye, while retinas isolated from the left eye were used for control measurements (Figure 4A). The levels of pri-miRNAs and mature miRNAs were measured at time points corresponding to the established minimal (dark adaptation, 90 min) and maximal (light adaptation, 30 min) levels of miRNAs (Figure 4B). Injection of α-Am (Figures 4C–4F and Figures S5C–S5E, left panels) or ActD (middle panels) completely blocked the increase of pri-miRNA and miRNA levels upon exposure to light, while the expected changes occurred in the control eye. In the presence of inhibitors, the pri-miRNAs and mature miRNAs remained at the low levels characteristic of a DA retina. Notably, upon repression of transcription the levels of mature miRNAs which do not undergo light-mediated regulation (let-7b and miR-29c) and their precursors also decreased dramatically (Figures 4E and 4F), indicating that many, if not all, miRNAs expressed in the retina may turnover rather rapidly.

Several control experiments were performed to demonstrate that the observed effects were indeed due to the action of injected inhibitors. As expected, the inhibitors blocked expression of the pol II-transcribed *Gαt1* mRNA but had no effect on expression of U6 snRNA, a stable pol III transcript (Figures S5F and S5G). Moreover, injection of only a buffer to the test eye had no effect on the level of any investigated RNA (Figures 4C–4F and Figures S5C–S5G, right panels).

We further investigated the turnover of selected miRNAs in LCM-dissected retinal layers of wild-type mouse or in specific cell types obtained by fluorescence activated cell sorting (FACS) from retinas of transgenic mice expressing EGFP or RFP under control of cell-specific promoters. As for the whole retina, inhibition of transcription resulted in a marked decrease in all tested miRNAs (including those which are not light-regulated: let-7b, miR-29c, miR-15a, and miR-16) in each dissected retina layer (Figures 5A and 5B). Interestingly, all miRNAs were found to turn over fast in FACS-sorted amacrine cells but not in rod bipolar cells (Figures 5D and 5E; see Discussion). No rapid turnover of miRNAs was observed in the FACS-sorted population of Müller glia cells (Figure 5F).

Taken together, these data indicate that miRNAs turn over rapidly in many types of retinal neurons, but not in rod bipolar cells or Müller glia, and that fast turnover applies to both light-responsive miRNAs and miRNAs which do not undergo light-mediated regulation.

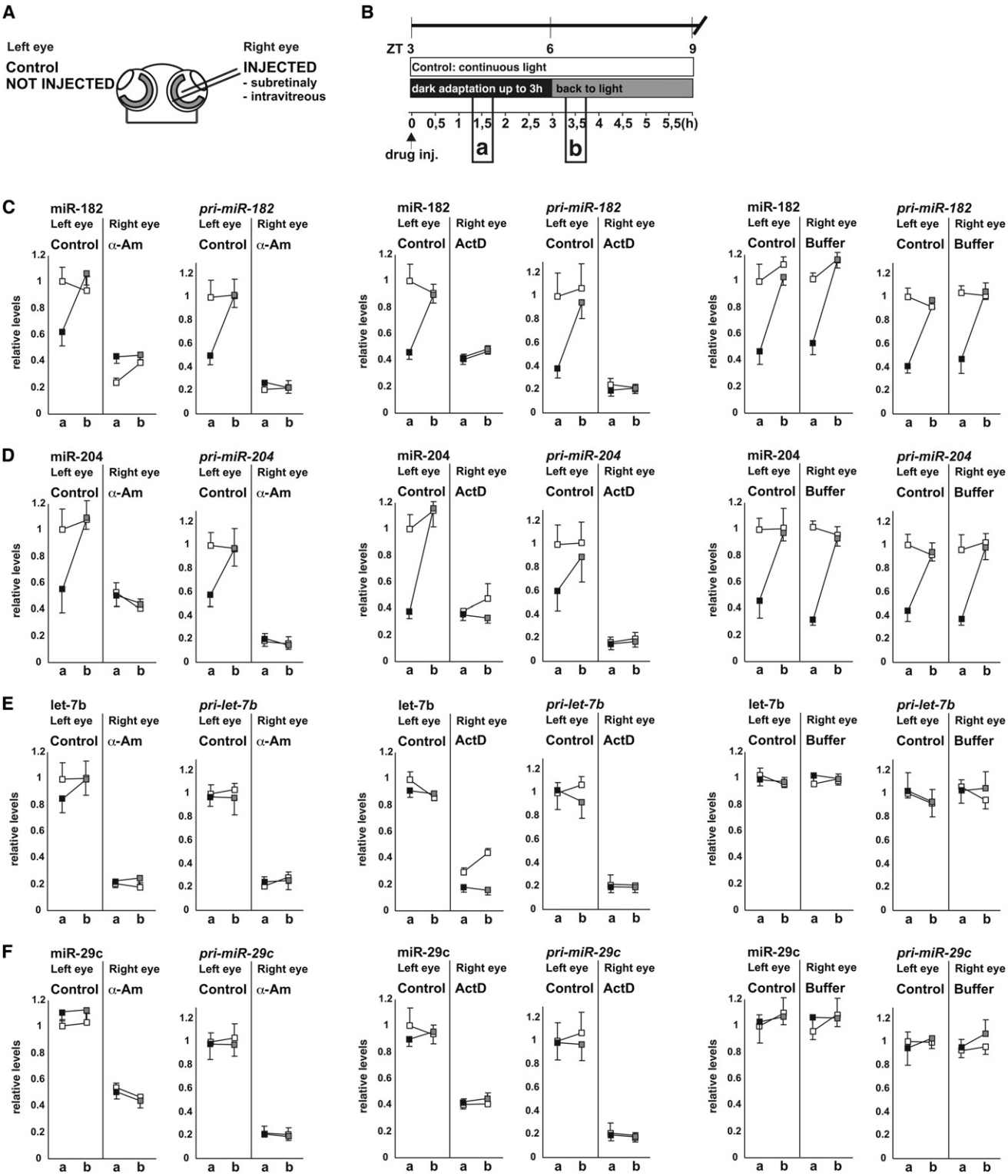

Figure 4. Effect of Transcription Inhibitors on miRNA and Pri-miRNA Levels in DA and LA Retinas

(A) Injections were performed into right eye, and the noninjected left eye was used for isolation of control retina.

(B) A scheme indicating time points used for collecting retinas.

(C–F) Effect of α-Am (left panels) and Act D (middle panels) on levels of indicated miRNAs and pri-miRNAs. Control determinations, for the noninjected left eye, are in the left subpanels. Levels of RNAs in retina from mice kept in continuous light, adapted to the dark for 90 min (a), or moved from dark to light for 30 min (b) are

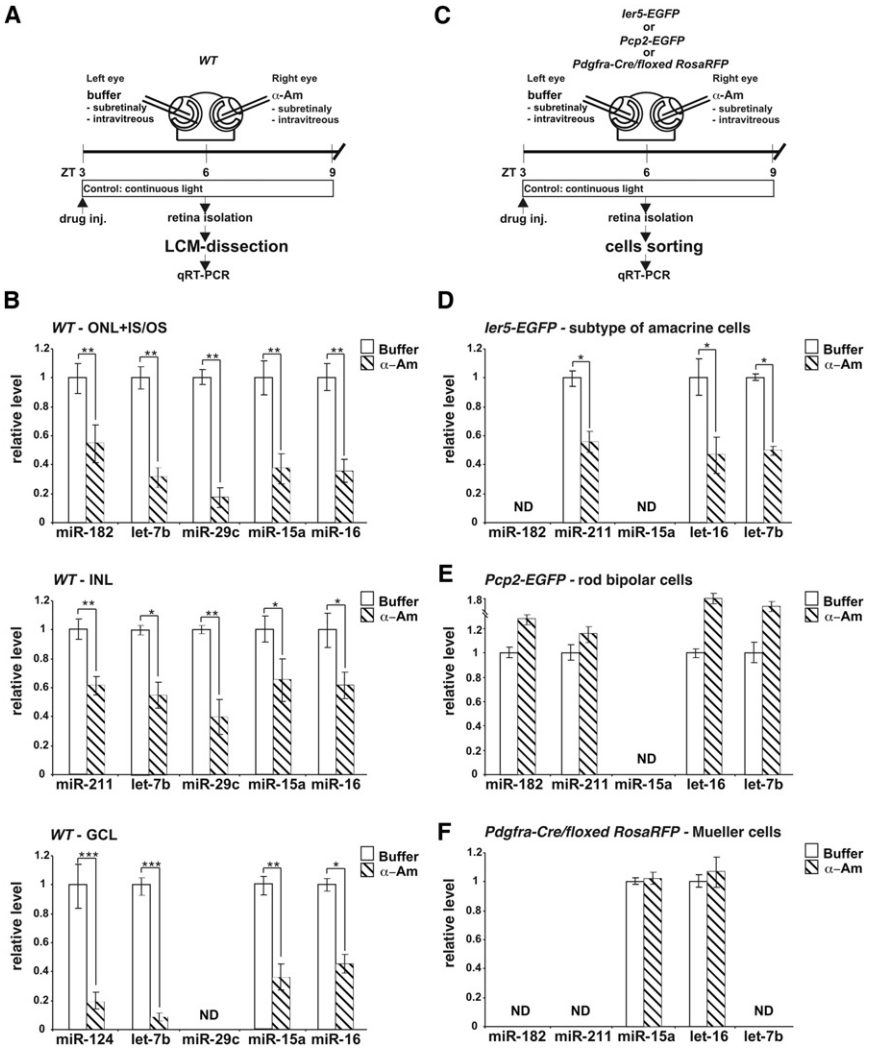

Figure 5. Determination of miRNA Turnover in LCM-Dissected Retinal Layers and FACS-Sorted Populations of Specific Retinal Cells

(A and C) Schemes indicating experimental approaches. Mice expressing either EGFP or RFP under control of cell-specific promoters are indicated in (C). Retinas were always isolated 3 hr after in vivo injection of either α-Am or a buffer.

(B) Effect of α-Am on the level of selected miRNAs in dissected ONL+OS/IS, INL or GCL layers of LA retinas. Values represent means ± SEM (n = 2; each RNA sample assayed in triplicate).

(D–F) miRNAs decay rapidly in amacrine cells (D) but not in rod bipolar (E) or Müller glia (F) cells of LA retinas. RNA was extracted from pools of FACS-sorted amacrine cells (~10,000 cells/pool; n = 2), a single pool of rod bipolar cells (~10,000 cells), or pools of Müller cells (~30,000 cells/pool; n = 2). Five animals were used for preparation of each pool. RNA from each pool was tested in triplicate. Values, normalized to U6 RNA, represent means ± SEM. Values for eyes injected with a buffer were set to one. ND, not detectable.

Fast Turnover of miRNAs Also Occurs in Nonretinal Neurons and Is Activity Dependent

The observed differences in the turnover of miRNAs between different retinal cell types and the fact that direct determination of miRNA decay was previously performed in only few studies, prompted us to measure miRNA catabolism in different cells and tissues. In all cases, the decay was determined using qRT-PCR, following treatment with either α-Am or ActD. Measurements performed with cultured NIH 3T3 and RPE-1 (human retinal pigmented epithelium) cells (Figures S7A–7D, left panels) and also nondifferentiated mouse embryonic stem (ES) cells (see Figure 7B) revealed no appreciable turnover of investigated miRNAs for 3 or 6 hr following the addition of transcription inhibitors; pri-miRNAs and urokinase (uPA) mRNA decayed rapidly, as expected (Figures S7A–S7D, right panels; Figure S7E).

To find out whether the fast turnover of miRNAs may be a general property of neuronal cells, we first measured the decay of miRNAs in rat brain cultured hippocampal slices (Stoppini et al., 1991) and dissociated hippocampal neurons (Schratt et al., 2004). In both systems, the addition of α-Am (Figures 6A and 6B; top panels) or ActD (data not shown) resulted in a marked decrease in the level of neuron-specific miRNAs miR-124, -128, -134, and -138. However, levels of another neuron-enriched miRNA, miR-132, and miRNAs known to be either ubiquitously expressed or enriched in glial cells (miR-16, 23a/b, -25, -29c, -193a; Landgraf et al., 2007) were not markedly affected. Similar rapid decay of many miRNAs was also observed in mouse cultured cortical neurons (Figure 6C). We note that, in most instances, the levels of mature neuronal miRNAs decreased only ~2-fold, indicating that either only part of the cellular miRNA pool is accessible to the degradation, or that miRNAs turn over rapidly only in a fraction of neurons (see Discussion). As expected, pri-miRNAs underwent fast degradation no matter whether they were precursors to neuronal or nonneuronal miRNAs (Figures 6A–6C).

Interestingly, in all three investigated cultures the inclusion of tetrodotoxin (TTX), a toxin which blocks sodium channels and neuronal action potentials, prevented rapid turnover of miRNAs (Figure 6, panels +TTX +α-Am). Incubation with TTX in the absence of transcription inhibitors had no effect on miRNA levels (Figure 6,

shown as white, black, and gray squares, respectively. Values, normalized to either U6 RNA (for α-Am and buffer injections) or 18S rRNA (for ActD injections) are means ± SEM; n = 3. Values for retinas from the control eye of mice kept in continuous light (time-point a) were set to one.
See also Figure S5.

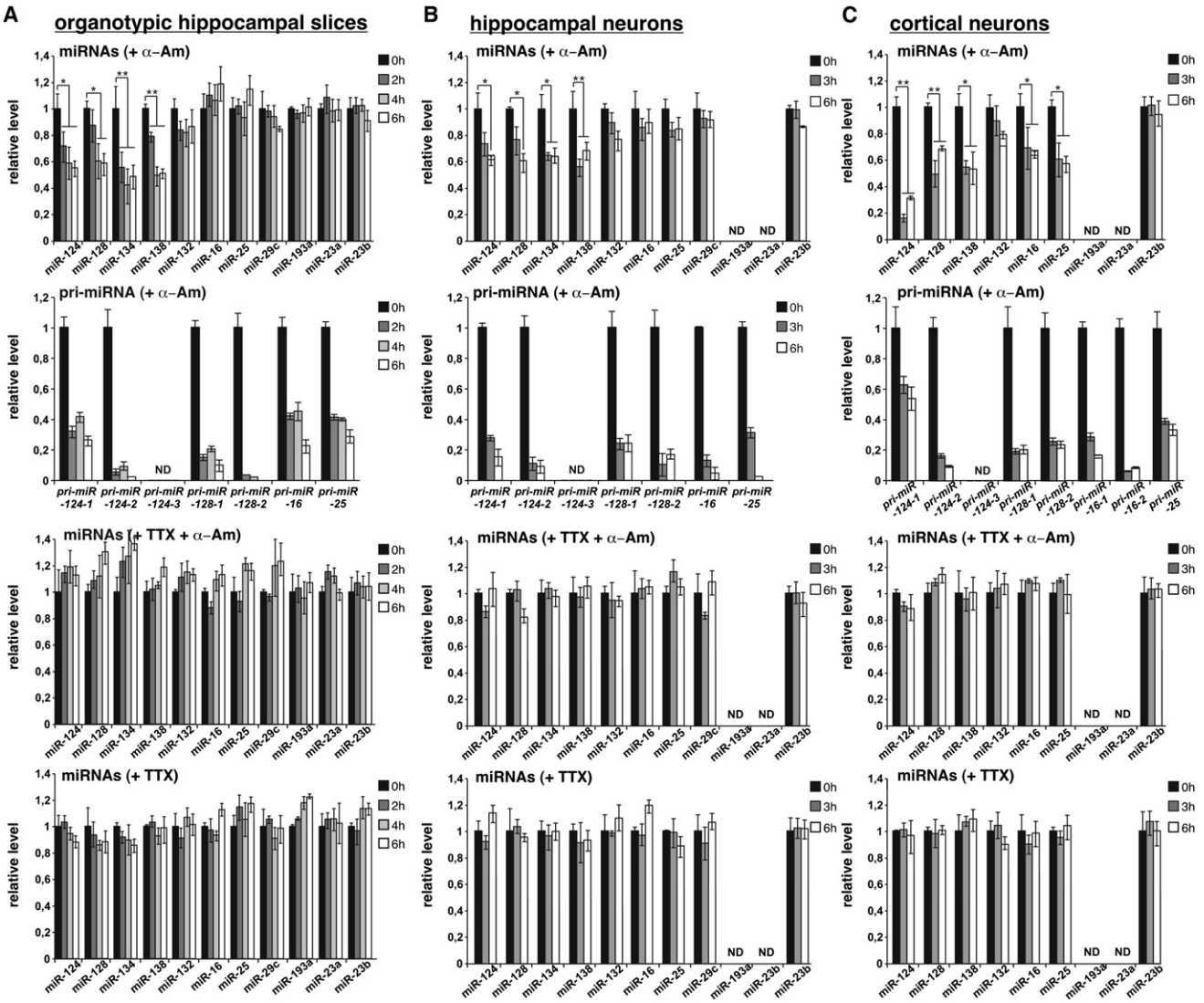

Figure 6. Activity-Dependent Decay of miRNAs in Different Types of Neurons

(A) Organotypic hippocampal slices.

(B) Dissociated hippocampal neurons (DIV12).

(C) Dissociated neocortical neurons (DIV25).

Levels of mature miRNAs (upper and two bottom rows) or pri-miRNAs (second row) were determined using RNA from cultures treated for the indicated times with α-Am or TTX alone, or a mixture of both. TTX was added to hippocampal slices and cultured neuron, 1.5 and 0.5 hr prior to the addition of α-Am, respectively. Values, normalized for U6 RNA, are means ± SEM ($n \geq 3$), with controls at 0 hr set to one. Note that in cortical neuron preparations, the nonneuron specific miRNAs (miR-16 and -25) also show accelerated turnover. ND, not detectable.

See also Figure S6.

panels +TTX). We have verified that TTX is unlikely to affect the transcription of miRNA genes since its inclusion had no effect on pri-miRNA levels in any system (Figures S6A–S6C). Likewise, TTX had no apparent effect on the processing or turnover of pri-miRNAs (Figures S6A–S6C). These results also argue against TTX having any effect on the action of α-Am as transcription inhibitor. Analysis of hippocampal slices and dissociated neurons treated with α-Am or α-Am+TTX, by either staining with calcein AM (CalAM; staining live cells) and ethidium homodimer-1 (EthD-1; staining dead cells) or counting apoptotic nuclei, indicated that toxic effects of the inhibitors were very limited (Figures S6D and S6E). This argues against a possibility that the observed reductions in miRNA levels are results of selective neuronal loss upon inhibitor treatment. In summary, our data indicate that accelerated turnover of miRNAs in neurons is dependent on their activity.

Activity-Dependent Turnover of miRNAs in Neurons Derived from ES Cells

To obtain additional evidence that miRNAs turn over faster in neurons than in nonneuronal cells, we used an in vitro system

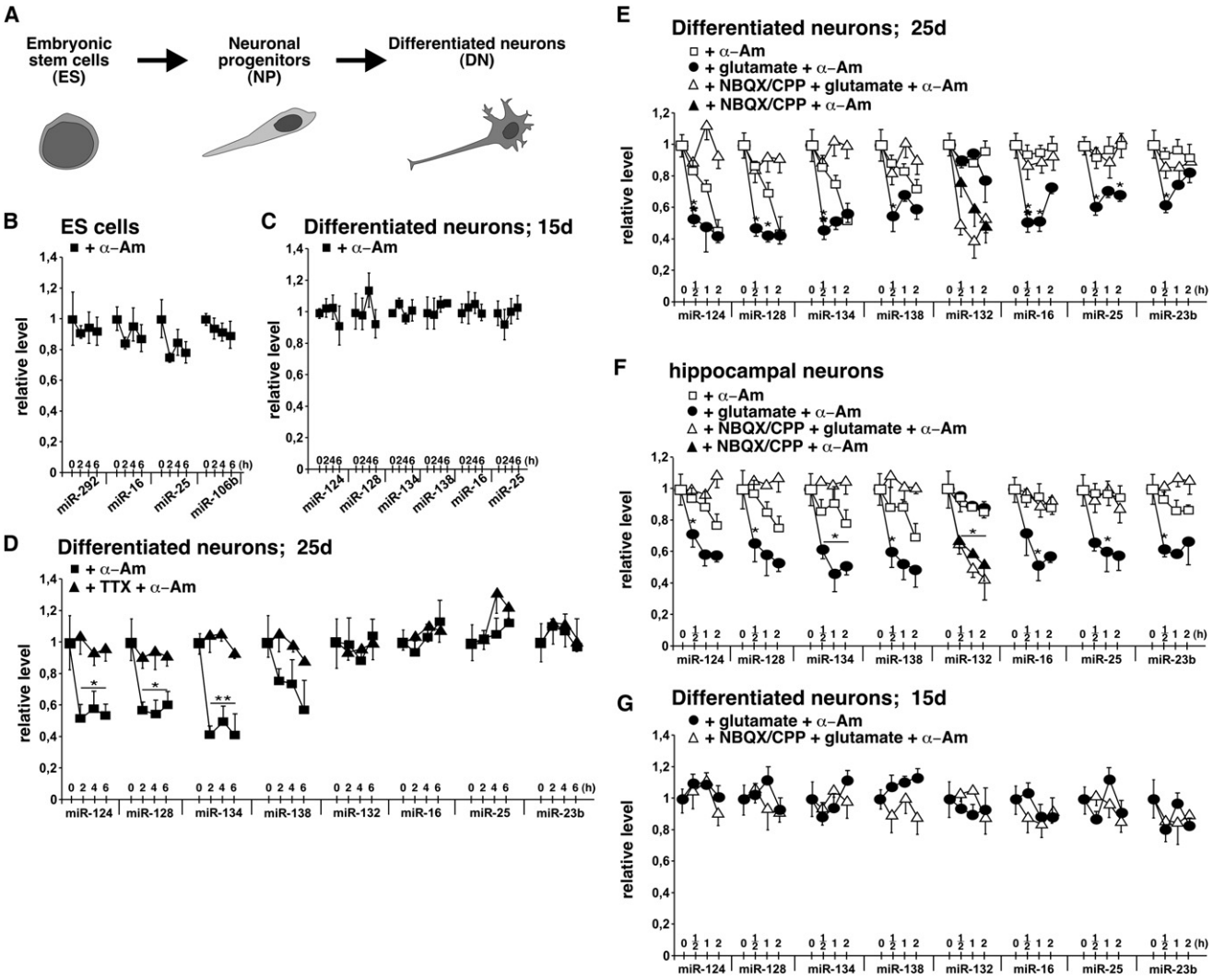

Figure 7. Analysis of Turnover of miRNAs in Mouse ES Cells and Neurons Derived from Them

(A) Scheme of the in vitro differentiation of mouse ES cells into neuronal progenitors (NP) and neurons (DN).

(B–D) Effect of α-Am or TTX + α-Am on the level of indicated miRNAs in ES cells or neurons maintained in culture for 15 or 25 days.

(E–G) Effect of α-Am, glutamate + α-Am, or NBQX/CPP + glutamate + α-Am on the level of miRNAs in ES-cell-derived neurons (E and G) and hippocampal neurons (F). For cultures treated with NBQX/CPP and α-Am (black triangles), only miR-132 level measurements are shown in panels E and F. Levels of other miRNAs were not affected by this treatment (not shown). Glutamate and/or NBQX/CPP were added to cultures 15 min prior to the addition of α-Am. Following α-Am addition, cultures were collected at indicated times (0–6 hr for panels B–D; 0–2 hr for panels E–G). Values, normalized for U6 RNA, are means ± SEM (n = 4). See also Figure S7.

in which mouse ES cells are differentiated into a population of glutamatergic neurons. In this system, ES cells are first differentiated into neural progenitors (NPs) characterized as radial glial cells, which then give rise to differentiated pyramidal neurons (DNs; Figure 7A), known to form functional synaptic connections (Bibel et al., 2004). We found that in nondifferentiated ES cells (Figure 7B), NPs (not shown), and DNs maintained in culture for 15 days (Figure 7C), miRNAs did not show any appreciable turnover during the 6 hr following the α-Am addition (Figures 7B and 7C) or ActD (data not shown); as expected, pri-miRNAs and uPA mRNA turned over rapidly in these cells (Figures S7E and S7F). In marked contrast to the 15 day culture, in neurons cultured for 25 days neuronal miRNAs miR-124, -128, -134, and -138 turned over rapidly, and their turnover was blocked by TTX; in contrast, no significant changes in the level of miR-132, and constitutive miRNAs miR-16, -23b, and -25b were seen (Figure 7D). In control experiments, we have verified that the pri-miRNA levels decreased in 25 day cultures in the presence of α-Am with similar kinetics irrespective of TTX being added to the assays (Figure S7G). Moreover, addition of α-Am and/or TTX (or glutamate and/or NBQX/CPP; see below) did not result in a substantial cell death, particularly when cells were treated with inhibitors for 2 hr (Figure S7H), sufficient time to reach maximal changes in miRNA levels (Figure 7D). We

also ascertained that the observed changes in miRNA levels were not due to changes in levels of Dicer or Argonaute-2 (AGO2), proteins required for miRNP assembly; treatment with α-Am or α-Am + TTX had no effect on levels or electrophoretic mobility of these proteins in 25 day ES-cell-derived or hippocampal neurons (data not shown).

The ES-cell-derived neurons express glutamate receptors and respond to glutamate stimulation (Bibel et al., 2004). Thus, we tested whether glutamate has an effect on miRNA turnover in neurons cultured for 25 days. Blocking glutamate receptors with NBQX/CPP (6-nitro-2,3-dioxo-1,4-dihydrobenzo[f]quinoxaline-7-sulfonamide, blocking AMPA and kainate receptors, plus (±)-3-(2-carboxypiperazin-4-yl)propyl-1-phosphonic acid, blocking NMDA receptors) prevented turnover of miR-124, -128, -134, and -138 but, surprisingly, activated decay of miR-132, which did not show any turnover in control neurons (Figure 7E). In contrast, the addition of glutamate markedly accelerated decay of miR-124, -128, -134, and -138, and also made constitutive miRNAs decay at an appreciable rate; inclusion of NBQX/CPP blocked the effect of exogenous glutamate (Figure 7E). Notably, miR-132 again showed an opposite trend. Its degradation was accelerated on the blocking of glutamate receptors and not by treatment with glutamate. Identical results were obtained with dissociated hippocampal neurons (Figure 7F).

We have also tested whether glutamate can induce the decay of miRNAs in ES-cell-derived neurons cultured for 15 days. The addition of glutamate, or NBQX/CPP plus glutamate, had no effect on the turnover of any miRNA (Figure 7G). To follow the electrophysiological properties of the ES-cell-derived neurons as a function of time in culture, we cultured them on microelectrode arrays (MEAs) and recorded their spontaneous spiking activity. Although some spiking was already visible after 10 to 15 days, maximal activity was reached after 25–30 days of culturing (Figure S7I).

In summary, these experiments indicate that in both ES-cell-derived and hippocampal neurons neuronal activity may have both stimulatory and inhibitory effects on miRNA turnover. Experiments with differentiated ES cells also suggest that neurons have to reach a certain level of maturity or connectivity to manifest activity-dependent changes in miRNA decay.

DISCUSSION

In this work, we identified miRNAs which respond to different light conditions in mouse retinal neurons, independent of the circadian clock. Levels of the sensory neuron-specific miR-183/96/182 cluster, and miR-204 and -211, were downregulated during dark adaptation and upregulated during light adaptation, with rapid miRNA decay and increased transcription being responsible for the respective changes. We identified the voltage-dependent glutamate transporter, *Slc1a1*, as one of the targets of the light-regulated miR-183/96/182 cluster; other likely targets of these miRNAs in photoreceptor cells include *Paip2b* and *Atp1b3*. We found that many miRNAs in retinal, and also nonretinal, neurons turn over much faster than miRNAs in other cell types. Blocking action potentials with TTX, or glutamate receptors with NBQX/CPP, strongly affected miRNA turnover rates, indicating that active miRNA metabolism may be important for the function of neurons.

Different algorithms were previously used to predict targets of miRNAs expressed in the retina, and, in a few instances, the validity of the predictions was tested using 3′-UTR reporter fusions in HEK293 or NIH 3T3 cells overexpressing retinal miRNA mimics (Arora et al., 2007; Xu et al., 2007). Using three different algorithms, we compiled a list of potential miR183/96/182 targets, including 214 mRNAs expressed in the mouse retina. Levels of 12 of them were up by more than 2-fold ($p < 0.05$) in the photoreceptor layer of the DA retina as compared to the LA retina, consistent with the decrease in miR-183/96/182 miRNAs in the dark.

For mRNA encoding SLC1A1, we obtained compelling evidence that it is a bona fide target of miR-183/96/182 miRNAs. In addition to the support obtained from reporter assays, performed in vitro and in vivo, we found that: (1) the AAV-mediated expression of "sponges," which titrate miR-183/96/182 miRNAs in photoreceptors in vivo, resulted in a marked increase in the SLC1A1 level in the LCM-dissected photoreceptor layer; and, (2) in the western blot analyses, the level of SLC1A1 increased 2- to 3-fold during dark adaptation, an effect expected to accompany the decrease in miR183/96/182 in the dark. Experiments listed in (1) and (2), indicated that also *Paip2b* and *Atp1b3* are likely to represent miR183/96/182 targets. To our knowledge, *Slc1a1*, *Paip2b*, and *Atp1b3* represent the first examples of miRNA-regulated mRNAs documented in the physiological context of the retina.

The finding that *Slc1a1*, which encodes a neuronal glutamate transporter, is a target of the miR-183/96/182 cluster, and that its level increases in the dark, is intriguing. Glutamate is the neurotransmitter used by vertebrate photoreceptors (Copenhagen and Jahr, 1989). In the dark, photoreceptors are depolarized and release glutamate. Light hyperpolarizes the membrane and the release of glutamate is reduced. It has been shown that glutamate transporters help to clear glutamate from the synaptic cleft in rods and cones (Gaal et al., 1998; Hasegawa et al., 2006). In the DA state, the load on rod glutamate transporters is higher than in the LA state, when rods are saturated by light, and therefore the upregulation of glutamate transporters in the dark may help to scavenge glutamate from the synaptic cleft. In LA retinas, when SLC1A1 expression of is low (Figures 2B and 2D), it has been suggested (Hasegawa et al., 2006) that the glutamate transporter in rods is SLCA1A7. However, immunohistochemical evidence shows that SLC1A1 is also present in rods (Kugler and Beyer, 2003). We propose that SLCA1A1 in the dark helps SLC1A7 to remove glutamate from the first visual synapse.

Kinetic experiments and the use of transcription inhibitors have revealed that all tested miRNAs, both light-regulated and constitutively expressed, decay in retinal neurons very rapidly ($T_{1/2}$ of 1h or less). This contrasts with the situation in purified Müller glia and rod bipolar cells, in which no decrease in the level of miRNAs was observed during 3 hr of α-Am treatment. Inhibitor experiments also indicated that fast upregulation of miR-183/96/182, miR-204 and -211 levels upon exposure to light is due to increased transcription of the respective genes. It is important to emphasize that, while turnover experiments with nonretinal neurons involved the use of α-Am or ActD, the rapid decay of miRNAs in the retina in vivo was observed upon transfer of animals from light to dark, thus under physiological conditions, in the absence of the inhibitors.

Rapid decay of many miRNAs was also observed in cultured rodent neurons or hippocampal slices, and in neurons differentiated from mouse ES cells in vitro. In all these systems, the addition of α-Am or ActD resulted in a rapid decrease in the level of neuron-specific miRNAs such as miR-124, -128, -134, and -138, In contrast, we observed no appreciable decay of miRNAs over 6 hr in cultured NIH 3T3, RPE-1 or ES cells. Experiments with neurons indicated that miRNA turnover may be subject to complex activity-dependent regulation. In all four neuronal cultures investigated, blocking action potentials with TTX prevented rapid turnover of miRNAs. Blocking glutamate receptors with NBQX/CPP likewise prevented turnover of miR-124, -128, -134, and -138 in hippocampal and ES-cell-derived neurons, while the addition of glutamate accelerated it. Notably, the behavior of miR-132 was opposite to the other miRNAs. Its degradation was induced by the blocking of glutamate receptors and not by the addition of glutamate. miR-132 represents one of the most studied neuronal miRNAs. Its transcription is upregulated by light and it modulates the expression of clock genes in the superchiasmatic nucleus in mice (Cheng et al., 2007). Importantly, the expression of miR-132 is activated in response to neuronal stimulation in rodent brain or culture neurons (Wayman et al., 2008; Nudelman et al., 2009), and miR-132 is required for activity-dependent dendritic growth and spine formation (Wayman et al., 2008; Impey et al., 2010). These findings, clearly distinguishing the activity of miR-132 from that of miRNAs such as miR-134 or -138, which generally reduce dendritic spine growth (reviewed by Schratt, 2009), provide a possible rationale explaining why miR-132, in contrast to miR-134 or -138, is not a subject of the accelerated decay in active neurons.

The dependence of miRNA decay on neuronal activity may also explain why miRNAs were found to turn over fast in FACS-sorted amacrine cells but not rod bipolar cells. Rod bipolar cells are thought to be inactive during daylight conditions, while amacrine cells are activated during both dark and light states (Wässle, 2004). Since both types of cells were collected during daylight, it is likely that rod bipolar cells were less, or not at all, active. The observation that miRNAs decay fast in ES-cell-derived neurons cultured for 25 but not 15 days is also consistent with the idea that a defined level of neuronal maturation or connectivity is essential for increased catabolism of miRNAs. The MEA recordings showed that spontaneous spiking activity of 25 day neurons is substantially higher than that of 15 day neurons. In addition, we found that neither NBQX/CPP nor glutamate had any effect on miRNA decay in 15 day cultures.

Rajasethupathy et al. (2009) reported recently that levels of two miRNAs, miR-124 and -184, are downregulated 2- to 3-fold in *Aplysia* neurons upon stimulation with serotonine, although no inhibitor studies were performed to determine the mechanism involved. In another recent report, Sethi and Lukiw (2009) found that brain-enriched miRNAs in human primary neural cultured cells and postmortem brain tissues have a $T_{1/2}$ of 1-3.5h. Hence, rapid and/or activity-regulated miRNA decay may be a general feature of neurons. This contrasts with the situation in nonneuronal cells in which miRNAs generally turn over very slowly (Bhattacharyya et al., 2006; Hwang et al., 2007; this work), with estimated half-lives extending even beyond 24 hr (Gatfield et al., 2009).

What could be a role of accelerated turnover of miRNAs in neurons, and why would turnover be dependent on neuronal activity? Several hundred protein-coding genes have been identified in cortical and hippocampal neurons whose transcription is regulated by neuronal activity. Many of them encode transcription factors while others specify proteins with important functions in dendrites and synapses (reviewed by Flavell and Greenberg, 2008). Possibly, the rapid turnover of miRNAs and, consequently, a continuous supply of de novo-transcribed miRNAs, are prerequisites for the assembly of new miRNPs, which would be available for regulating the newly-synthesized activity-dependent mRNA targets. Such regulation might involve not only translation or stability of the targeted mRNAs, but also their localization and expression in neuronal processes (Schratt 2009). Blocking neuronal activity would make the need for rapid miRNA metabolism obsolete because of the diminished supply of potential mRNA targets. In another scenario, the fast decay of miRNAs might by important for stimulating translation of neuronal mRNAs, e.g., those located at dendritic spines, in response to synaptic activity (reviewed by Kosik, 2006; Schratt 2009).

In the future, it will be important to establish what factors are responsible for the rapid decay of miRNAs and its regulation in neurons. Enzymes responsible for miRNA turnover are beginning to be identified (Ramachandran and Chen, 2008; Chatterjee and Grosshans, 2009). In addition, the first examples of regulated miRNA turnover, such as differences in the miR-29b half-life between cycling and mitotic HeLa cells (Hwang et al., 2007), or the stabilizing effect of the A residue addition to the 3′end of miR-122 in liver (Katoh et al., 2009), have already been reported.

EXPERIMENTAL PROCEDURES

Light/Dark Adaptation of Mice and Retina Isolation

C57BL/6 mice were obtained from RCC (Fullinsdorf, Switzerland). Unless indicated otherwise, 6- to 8-week-old animals were used for the experiments. LA animals were kept in a room at 450 lux. For dark adaptation, animals were kept in a dark chamber with a maximum of 0.4 lux. Retinas from DA mice were isolated under dim red light.

Laser Capture Microdissection

For extraction of RNA from laser capture microdissection (LCM) dissected layers, isolated retinas were cryoprotected in 20% sucrose for 15 min and embedded in Shandon M-1 (Thermo Fisher) embedding matrix to 20% sucrose ratio 1:2. Frozen tissues were cut into 18 μm thick sections and mounted on RNase-free MMI (Molecular Machines & Industries AG) membrane slides. For RNA isolation, retinal sections from 5 mice were stained with Mayer's hematoxylin for 5 s, fixed, and dehydrated for 50 s in 100% ethanol. After the sections were briefly air dried, ~50,000 cells were captured from each retinal cell layer using MMI CellCut Plus System microscopy. Total RNA was extracted from captured cell layers using Trizol reagent. For protein analysis by western blotting, retinas were cryoprotected in 20% sucrose containing 10 μg/ml DAPI and embedded as described above. Sections were fixed and dehydrated in ice-cold methanol for 50 s. Once the sections were briefly air dried, ~100,000 cells were captured from each retinal layer, lysed in 1× lysis buffer containing 50 mM Tris, (pH 7.5), 10 mM EDTA, 1% SDS, and 1× protease inhibitor cocktail (Roche). For retinas infected with AAV2-Rho-EGFP/triple sponge or AAV2-Rho-EGFP/control viruses, ~50,000 cells from the EGFP-fluorescence-positive ONL+OS/IS layers were captured and lysed.

In Vivo Retina Electroporation and Two-Photon Ratiometric Imaging

Subretinal injection and in vivo electroporation of plasmids into newborn (P0 or P1) mouse pups was as described by Matsuda and Cepko (2004). A two-photon microscope (custom in-house design by J.D. and B.R.) equipped with a 60× water immersion lens (0.90W, LUMPlanFI/IR, Olympus, Japan) was used for ratiometric EGFP/RFP imaging.

Cell and Organotypic Tissue Cultures

Organotypic hippocampal slices were prepared from Wistar rats at postnatal day 5 (Stoppini et al., 1991). 25-day-old cultures were used for all experiments. Primary hippocampal neurons were prepared from E18.5 Sprague-Dawley rats and cultured on plates coated with laminin (Schratt et al., 2004). They were maintained in culture for 12 days in Neurobasal Medium (Invitrogen) supplemented with B27 (Invitrogen), 0.5 mM L-glutamine, and antibiotics. Mouse neocortical primary neurons were isolated from E16.5 C57Bl/6 mouse embryos and cultured for 28 days in serum-free medium, and supplements on dishes coated with poly-DL-ornithine.

ES cells, derived from blastocysts (3.5 PC) of mixed 129-C57BL/6 background mice, were cultured on feeder and subsequently without feeder of MEF cells, using 3i medium. Differentiation was performed essentially as described previously (Bibel et al., 2004) and cells were collected either 15 or 25 days after embryoid bodies dissociation.

Treatment with Inhibitors

For testing the effect of inhibitors on RNA metabolism in retina, animals maintained under 12 hr light/dark photoperiods were anesthetized and one of the eyes was injected both subretinally and intravitreously with 2 μl of 200 μM α-Am or ActD (Weiler et al., 1998) in 1× PBS containing 1% DMSO. The inhibitors were injected 10 min before initiating light/dark adaptation experiments (see Figures 4A and 4B and Figures S5A and S5B.

Organotypic hippocampal slices and cell cultures were treated with α-Am or ActD (both at 10 μg/ml; Sigma) for indicated time. To block voltage-dependent Na^+-channels, TTX (LATOXAN, France) was added to the medium at final concentration of 1 μM either 1.5 hr (organotypic slices) or 0.5 hr (cell cultures) prior to blocking of transcription. To block ionotropic glutamate receptors, NBQX (10 μM, Sigma) plus CPP (10 μM, Sigma) were used. Glutamate was added to the medium at final concentration of 10 μM (Bibel et al., 2004), 15 min prior to blocking of transcription.

SUPPLEMENTAL INFORMATION

Supplemental Information includes Extended Experimental Procedures, Supplemental References, seven figures, and three tables and can be found with this article online at doi:10.1016/j.cell.2010.03.039.

ACKNOWLEDGMENTS

We thank K. J. Sweadner and N. Sonenberg for antibodies; B. Gross Scherf, S. Djaffer, D. Gerosa Erni, and T. Wüst for excellent technical help; E. Oakeley for array analysis; and E. Cabuy, H. Kohler, and K. Jacobeit for help with LCM, FASC, and sequencing. We also thank members of W.F. and B.R. groups for valuable discussions. The work done in the laboratory of W.F. is supported by the EC FP6 Program "Sirocco." J.K. is the recipient of an EMBO Fellowship. V.B. and B.R. are supported by a fellowship and grant, respectively, from National Centers of Competence in Research, Frontiers in Genetics. The Friedrich Miescher Institute is supported by the Novartis Research Foundation.

Received: June 16, 2009
Revised: January 22, 2010
Accepted: March 5, 2010
Published: May 13, 2010

REFERENCES

Arora, A., McKay, G.J., and Simpson, D.A.C. (2007). Prediction and verification of miRNA expression in human and rat retinas. Invest. Ophthalmol. Vis. Sci. *48*, 3962–3967.

Bartel, D.P. (2009). MicroRNAs: targets recognition and regulatory functions. Cell *136*, 215–233.

Bhattacharyya, S.N., Habermacher, R., Martine, U., Closs, E.I., and Filipowicz, W. (2006). Relief of microRNA-mediated translational repression in human cells subjected to stress. Cell *125*, 1111–1124.

Bibel, M., Richter, J., Schrenk, K., Tucker, K.L., Staiger, V., Korte, M., Goetz, M., and Barde, Y.A. (2004). Differentiation of mouse embryonic stem cells into a defined neuronal lineage. Nat. Neurosci. *7*, 1003–1009.

Bushati, N., and Cohen, S.M. (2007). MicroRNA functions. Annu. Rev. Cell Dev. Biol. *23*, 175–205.

Chatterjee, S., and Grosshans, H. (2009). Active turnover modulates mature microRNA activity in Caenorhabditis elegans. Nature *461*, 546–549.

Cheng, H.Y., Papp, J.W., Varlamova, O., Dziema, H., Russel, B., Curfman, J.P., Nakazawa, T., Shimizu, K., Okamura, H., Imprey, S., and Obrietan, K. (2007). microRNA modulation of circadian-clock period and entrainment. Neuron *54*, 813–829.

Copenhagen, D.R., and Jahr, C.E. (1989). Release of endogenous excitatory amino acids from turtle photoreceptors. Nature *341*, 536–539.

Demb, J.B. (2008). Functional circuitry of visual adaptation in the retina. J. Physiol. *586*, 4377–4384.

Ding, X.C., Weiler, J., and Grosshans, H. (2009). Regulating the regulators: mechanisms controlling the maturation of microRNAs. Trends Biotechnol. *27*, 27–36.

Ebert, M.S., Neilson, J.R., and Sharp, P.A. (2007). MicroRNA sponges: competitive inhibitors of small RNAs in mammalian cells. Nat. Methods *4*, 721–726.

Filipowicz, W., Bhattacharyya, S.N., and Sonenberg, N. (2008). Mechanism of post-transcriptional regulation by microRNAs: are the answers in sight? Nat. Rev. Genet. *9*, 102–114.

Flavell, S.W., and Greenberg, M.E. (2008). Signaling mechanisms linking neuronal activity to gene expression and plasticity of the nervous system. Annu. Rev. Neurosci. *31*, 563–590.

Fu, Y., and Yau, K.W. (2007). Phototransduction in mouse rods and cones. Pflugers Arch. *454*, 805–819.

Gaal, L., Roska, B., Picaud, S.A., Wu, S.M., Marc, R., and Werblin, F.S. (1998). Postsynaptic response kinetics are controlled by a glutamate transporter at cone photoreceptors. J. Neurophysiol. *79*, 190–196.

Gatfield, D., Le Martelot, G., Vejnar, C.E., Gerlach, D., Schaad, O., Fleury-Olela, F., Ruskeepää, A.L., Oresic, M., Esau, C.C., Zdobnov, E.M., and Schibler, U. (2009). Integration of microRNA miR-122 in hepatic circadian gene expression. Genes Dev. *23*, 1313–1326.

Hasegawa, J., Obara, T., Tanaka, K., and Tachibana, M. (2006). High-density presynaptic transporters are required for glutamate removal from the first visual synapse. Neuron *50*, 63–74.

Hwang, H.-W., Wentzel, E.A., and Mendell, J.T. (2007). A hexanucleotide element directs microRNA nuclear import. Science *315*, 97–100.

Impey, S., Davare, M., Lasiek, A., Fortin, D., Ando, H., Varlamova, O., Obrietan, K., Soderling, T.R., Goodman, R.H., and Wayman, G.A. (2010). An activity-induced microRNA controls dendritic spine formation by regulating Rac1-PAK signalling. Mol. Cell. Neurosci. *43*, 146–156.

Karali, M., Peluso, I., Marigo, V., and Banfi, S. (2007). Identification and characterization of microRNAs expressed in the mouse eye. Invest. Ophthalmol. Vis. Sci. *48*, 509–515.

Katoh, T., Sakaguchi, Y., Miyauchi, K., Suzuki, T., Kashiwabara, S., Baba, T., and Suzuki, T. (2009). Selective stabilization of mammalian microRNAs by 3′ adenylation mediated by the cytoplasmic poly(A) polymerase GLD-2. Genes Dev. *23*, 433–438.

Kosik, K.S. (2006). The neuronal microRNA system. Nat. Rev. Neurosci. *7*, 911–920.

Kugler, P., and Beyer, A. (2003). Expression of glutamate transporters in human and rat retina and rat optic nerve. Histochem. Cell Biol. *120*, 199–212.

Landgraf, P., Rusu, M., Sheridan, R., Sewer, A., Iovino, N., Aravin, A., Pfeffer, S., Rice, A., Kamphorst, A.O., Landthaler, M., et al. (2007). A mammalian microRNA expression atlas based on small RNA library sequencing. Cell *129*, 1401–1414.

Loscher, C.J., Hokamp, K., Kenna, P.F., Ivens, A.C., Humphries, P., Palfi, A., and Farrar, G.J. (2007). Altered retinal microRNA expression profile in a mouse model of retinitis pigmentosa. Genome Biol. *8*, R248.

Matsuda, T., and Cepko, C.L. (2004). Electroporation and RNA interference in the rodent retina in vivo and in vitro. Proc. Natl. Acad. Sci. USA *101*, 16–22.

Morgans, C.W., Zhang, J., Jeffrey, B.G., Nelson, S.M., Burke, N.S., Duvoisin, R.M., and Brown, R.L. (2009). TRPM1 is required for the depolarizing light response in retinal ON-bipolar cells. Proc. Natl. Acad. Sci. USA *106*, 19174–19178.

Nieoullon, A., Canolle, B., Masmejean, F., Guillet, B., Pisano, P., and Lortet, S. (2006). The neuronal excitatory amino acid transporter EAAC1/EAAT3: does it represent a major actor at the brain excitatory synapse? J. Neurochem. *98*, 1007–1018.

Nudelman, A.S., DiRocco, D.P., Lambert, T.J., Garelick, M.G., Le, J., Nathanson, N.M., and Storm, D.R. (2009). Neuronal activity rapidly induces transcription of the CREB-regulated microRNA-132, in vivo. Hippocampus *20*, 492–498.

Pugh, E.N., Jr., Nikonov, S., and Lamb, T.D. (1999). Molecular mechanisms of vertebrate photoreceptor light adaptation. Curr. Opin. Neurobiol. *9*, 410–418.

Rajasethupathy, P., Fiumara, F., Sheridan, R., Betel, D., Puthanveettil, S.V., Russo, J.J., Sander, C., Tuschl, T., and Kandel, E. (2009). Characterization of small RNAs in aplysia reveals a role for miR-124 in constraining synaptic plasticity through CREB. Neuron *63*, 803–817.

Ramachandran, V., and Chen, X. (2008). Degradation of microRNAs by a family of exoribonucleases in Arabidopsis. Science *321*, 1490–1492.

Ryan, D.G., Oliveira-Fernandes, M., and Lavker, R.M. (2006). MicroRNAs of the mammalian eye display distinct and overlapping tissue specificity. Mol. Vis. *12*, 1175–1184.

Schratt, G.M., Nigh, E.A., Chen, W.G., Hu, L., and Greenberg, M.E. (2004). BDNF regulates the translation of a selected group of mRNAs by a mammalian target of rapamycin-phosphatidylinositol 3-kinase-dependent pathway during neuronal development. J. Neurosci. *24*, 7366–7377.

Schratt, G. (2009). microRNAs at the synapse. Nat. Rev. Neurosci. *10*, 842–849.

Sethi, P., and Lukiw, W.J. (2009). Micro-RNA abundance and stability in human brain: Specific alteration in Alzheimer's disease temporal lobe neocortex. Neurosci. Lett. *459*, 100–104.

Shen, Y., Heimel, J.A., Kamerans, M., Peachey, N.S., Gregg, R.G., and Nawy, S. (2009). A transient receptor potential-like channel mediates synaptic transmission in red bipolar cells. J. Neurosci. *29*, 6088–6093.

Stoppini, L., Buchs, P.A., and Muller, D. (1991). A simple method for organotypic cultures of nervous tissue. J. Neurosci. Methods *37*, 173–182.

Tzingounis, A.V., and Wadiche, J.I. (2007). Glutamate transporters: confining runaway excitation by shaping synaptic transmission. Nat. Rev. Neurosci. *8*, 935–947.

Wässle, H. (2004). Parallel processing in the mammalian retina. Nat. Rev. Neurosci. *5*, 747–757.

Wayman, G.A., Davare, M., Ando, H., Fortin, D., Varlamova, O., Cheng, H.Y., Marks, D., Obrietan, K., Soderling, T.R., Goodman, R.H., and Impey, S. (2008). An activity-regulated microRNA controls dendritic plasticity by down-regulating p250GAP. Proc. Natl. Acad. Sci. USA *105*, 9093–9098.

Weiler, R., Schultz, K., Pottek, M., Tieding, S., and Janssen-Bienhold, U. (1998). Retinoic acid has light-adaptative effects on horizontal cells in the retina. Proc. Natl. Acad. Sci. USA *95*, 7139–7144.

Xu, S., Witmer, P.D., Lumayag, S., Kovacs, B., and Valle, D. (2007). microRNA (miRNA) transcriptome of mouse retina and identification of a sensory organ-specific miRNA cluster. J. Biol. Chem. *282*, 25053–25066.